Published in final edited form as:
Nat Immunol. 2016 March ; 17(3): 323–330. doi:10.1038/ni.3348.

Blimp-1 controls plasma cell function through regulation of immunoglobulin secretion and the unfolded protein response

Julie Tellier[1,2], **Wei Shi**[1,3], **Martina Minnich**[4], **Yang Liao**[1,2], **Simon Crawford**[5], **Gordon K Smyth**[1,6], **Axel Kallies**[1,2], **Meinrad Busslinger**[4], and **Stephen L Nutt**[1,2]

[1]The Walter and Eliza Hall Institute of Medical Research, 1G Royal Parade, Parkville, Victoria, 3052, Australia

[2]Department of Medical Biology, The University of Melbourne, Parkville, Victoria, 3010, Australia

[3]Department of Computing and Information Systems, The University of Melbourne, Parkville, Victoria, 3010, Australia

[4]Research Institute of Molecular Pathology (IMP), Vienna Biocenter (VBC), Dr. Bohr-Gasse 7, A-1030 Vienna, Austria

[5]School of BioSciences, The University of Melbourne, Parkville, Victoria, 3010, Australia

[6]Department of Mathematics and Statistics, The University of Melbourne, Parkville, Victoria, 3010, Australia

Abstract

Plasma cell differentiation requires silencing of B cell transcription, while establishing antibody-secretory function and long-term survival. The transcription factors Blimp-1 and IRF4 are essential for plasma cell generation, however their function in mature plasma cells has remained elusive. We have found that while IRF4 was essential for plasma cell survival, Blimp-1 was dispensable. Blimp-1-deficient plasma cells retained their transcriptional identity, but lost the ability to secrete antibody. Blimp-1 regulated many components of the unfolded protein response (UPR), including XBP-1 and ATF6. The overlap of Blimp-1 and XBP-1 function was restricted to the UPR, with Blimp-1 uniquely regulating mTOR activity and plasma cell size. Thus, Blimp-1 is required for the unique physiological capacity of plasma cells that enables the secretion of protective antibody.

Correspondence should be addressed to: S.L.N. (nutt@wehi.edu.au).

AUTHOR CONTRIBUTIONS

J.T. performed most experiments; W.S., Y.L. and G.K.S. performed the bioinformatic and statistical analyses; M.M. and M.B. provided ChIPseq data; S.C. performed electron microscopy; A.K. provided mouse models; S.L.N. supervised the study; J.T. and S.L.N. wrote the manuscript, to which all authors had editorial input.

ACCESSION CODES

Raw sequence reads, read counts and normalized expression values have been deposited into the GEO (Gene Expression Omnibus) database under accession number GSE70981.

COMPETING FINANCIAL INTERESTS

The authors declare no competing financial interests.

Europe PMC Funders Author Manuscripts

Keywords

plasma cell; unfolded protein response; mTOR; immunoglobulin; transcription factor

Europe PMC Funders Author Manuscripts

INTRODUCTION

The production of antibody is an essential arm of the immune response, providing both immediate protection against a current infection and long-term immunity against re-exposure to the same pathogen. The antibody-secreting cell (ASC) compartment consists of short-lived proliferating plasmablasts (PBs), which are generated early in an immune response, and long-lived post-mitotic plasma cells (PCs) that reside in specialized niches in the bone marrow (BM)[1,2]. These long-lived PCs have been shown to maintain high-titers of protective antibody for decades after pathogen exposure or immunization[3]. Thus understanding the factors that control PC production, function and long-term survival is critical for both improved vaccine design and to provide novel approaches to target pathogenic PCs in diseases such as multiple myeloma and systemic lupus erythematosus.

To achieve the dual goal of maintaining an extremely high rate of immunoglobulin secretion, while ensuring long-term survival, PCs show a highly specialized morphology with enlarged cytoplasm and tightly arranged endoplasmic reticulum (ER). PCs also constitutively activate the unfolded protein response (UPR), a specialized sensing mechanism to detect and deal with large amounts of protein passing through the ER[4].

The differentiation of activated B cells into PCs requires the coordinated change in the expression of many hundreds of genes, including the silencing of B cell-associated transcripts, including the transcription factors *Pax5*, *Bach2* and *Bcl6*, and the activation of a suite of PC-specific genes[5,6]. This developmental program is guided by a triad of transcription factors; IRF4, Blimp-1 (encoded by *Prdm1*) and XBP-1. IRF4 is both highly expressed and essential for PC development, at least in part due to its regulation of *Prdm1* (refs. 7-9). Blimp-1 is expressed in all ASCs and is also required for their differentiation beyond an early point[10-12]. Blimp-1 has to date been thought of as a transcriptional repressor, silencing several important B cell genes, including *Pax5* (ref. 13), *Myc*[14], *Ciita*[15], *Bcl6*, *Spib* and *Id3* (ref. 16), with only limited understanding of its targets in PCs [17]. XBP-1, an important component of the UPR, was initially proposed to the essential for PC formation[18], however, recent evidence suggests that XBP-1 is more specifically required for immunoglobulin production[19-22]. As a consequence of the important functions of IRF4 and Blimp-1 early in the differentiation process, there is little current knowledge about the function of these factors in long-lived PCs[23,24]. Here we have used a genetic approach to investigate the functional consequences of the loss of either IRF4, Blimp-1 or XBP-1 in mature post-mitotic BM PCs.

RESULTS

IRF4 and Blimp-1 inactivation in plasma cells

To assess the importance of IRF4 and Blimp-1 in mature BM PCs, we crossed mice carrying *lox*P-flanked (floxed) alleles encoding both genes[25,26] to *Rosa26*-Cre^{ERT2} mice[27]. This system allows the tamoxifen-inducible inactivation of *Irf4* or *Prdm1* in pre-existing PCs. To facilitate the tracking of PCs, *Prdm1*-floxed and control mice also carried a *Prdm1*^{GFP} reporter allele, which expressed green fluorescent protein (GFP) but no functional Blimp-1 (ref. 11), while *Irf4*-floxed mice carried an internal GFP cassette that reported gene inactivation[26]. We transferred B cells from these mice into B- and T cell-deficient *Rag1*$^{-/-}$ mice to generate a large population of PCs, and Cre activity was induced by tamoxifen administration 14 days later. Although inactivation of *Irf4* occurred equivalently in *Irf4*$^{fl/+}$ and *Irf4*$^{fl/-}$ in B cells (approximately 15% GFP^{+} cells in each genotype, data not shown), GFP^{+} PCs were lost from the BM, early as two days after tamoxifen treatment, demonstrating that IRF4 was indispensable for PC survival (Fig. 1a and Supplementary Fig. 1a). By contrast, inactivation of *Prdm1* using an identical strategy resulted in a PC population was that stable for many weeks after tamoxifen treatment (Fig. 1a and Supplementary Fig. 1a). To confirm this result, we induced *Prdm1* inactivation in intact naïve *Prdm1*$^{fl/gfp}$Cre^{ERT2} mice, and again found that BM PCs persisted without Blimp-1 (Fig. 1b and Supplementary Fig. 1b). Similar differential dependency of PC survival on IRF4 and Blimp-1 was observed in spleen (Supplementary Fig. 1a-d). Although both models showed a statistically significant reduction in PCs numbers at the latest time points after *Prdm1* inactivation, the data derived from the two genotypes are not strictly comparable, as the *Prdm1*$^{+/gfp}$ B cells continue to produce new PCs throughout the course of the experiment, while the *Prdm1*$^{fl/gfp}$ cells lack this capacity. Consistent with this conclusion, we observed no statistically significant change in proportion of *Prdm1*$^{fl/gfp}$ PCs, both in steady state and after immunization with a protein antigen in alum, over the time frame examined (Fig. 1a,b and Supplementary Fig. 1c–e). The efficiency of *Prdm1* ablation was assessed by treating *Rag1*$^{-/-}$ mice with tamoxifen two days after transfer, before PCs could be formed. This approach completely blocked PC differentiation, mimicking the conditional removal of *Prdm1* from activated B cells *in vitro* ([12,28], Supplementary Fig. 1f, 2a). PCR genotyping of purified B cells and PCs confirmed the efficient inactivation of the *Prdm1* locus in both cell types (Supplementary Fig. 2b). These data demonstrate that Blimp-1 was not essential for the long-term survival of bone marrow plasma cells.

Blimp-1 regulated genes in plasma cells

The long-term persistence of Blimp-1-deficient PCs enabled us to investigate the impact of Blimp-1 loss on the transcriptome of long-lived PCs. We performed RNA sequencing on BM PCs purified from *Prdm1*$^{fl/gfp}$Cre^{ERT2} and control *Prdm1*$^{+/gfp}$Cre^{ERT2} mice 21 days after tamoxifen treatment. Analysis of the frequency of *Prdm1* transcripts spanning exons 5-6, which are removed by the Cre-mediated excision of the floxed exon 5, revealed an 87% reduction in frequency of full-length transcripts in the *Prdm1*$^{fl/gfp}$Cre^{ERT2} samples, compared to the control *Prdm1*$^{+/gfp}$Cre^{ERT2} genotype (Supplementary Fig. 2c). 465 genes were differentially expressed (170 genes activated and 295 repressed by Blimp-1, normalized average expression ≥4 RPKM in at least one sample, False Discovery Rate

(FDR) ≤0.05 (Supplementary Table 1)) between control and Blimp-1-deficient PCs (Fig. 2a). Cross referencing these differentially expressed genes with Blimp-1 binding, as assessed by ChIPseq using a biotin-tagged *Prdm1* allele[29] in *in vitro*-generated PBs, revealed that 28% (47/170) of Blimp-1–activated and 41% (120/295) of Blimp-1–repressed genes were bound by Blimp-1, and were thus potential direct target genes (Supplementary Table 1). Partitioning of the proteins encoded by the differentially expressed genes into functional categories showed that the largest group of Blimp-1–activated genes encoded proteins involved in metabolism and nutrient transporters, whereas many genes that Blimp-1–repressed encoded receptors and signaling molecules (Fig. 2b). This analysis also suggested a role of Blimp-1 in inhibiting the B cell functions, including antigen presentation (MHCII molecules), pathogen recognition (*Tlr9*) and signaling through the activating receptors (*Cd79b, Bank1*). Concomitantly, Blimp-1 appeared important for the transcription of genes related to metabolic activity of the PC, most likely to adapt to its secretory function (*Tpst2, Syvn1, Fkbp11*). Interestingly, very few genes involved in cell cycle or survival were affected by Blimp-1 loss. For example, *Myc*, a known target of Blimp-1–mediated repression and central regulator of proliferation[14], was not re-expressed. The expression of essential players in PC survival, as *Mcl1* (ref. 30), *Bcl2l11* (encoding Bim) or *Tnfrsf17* ([31], encoding BCMA) remained similarly unchanged (Fig. 2c and data not shown).

As Blimp-1 has previously been implicated in the silencing of the B cell transcriptional program upon PC differentiation[16], we examined whether the BM PCs revert to the B cell stage without Blimp-1. Several B cell-associated genes, including *Cd22, Spib, Cd79b*, and *Ciita* were re-expressed in the absence of Blimp-1 (Fig. 2c). Most importantly, the genes encoding *Pax5* and *Bcl6*, two of the major regulators of the B cell transcriptome and known targets of Blimp-1 repression[13,16] were not re-expressed, demonstrating that the Blimp-1–deficient PCs were not reverting to the more developmentally immature B cell fate (Fig. 2c and data not shown). The absence of *Pax5* and *Bcl6* expression may also explain the only partial reactivation of the B cell genes such as those encoding CD22 and MHCII, compared to their expression in wild-type B cells (Fig. 2c,d). Blimp-1 was also required for the normal expression of some PC genes including CD93 (Fig. 2c,d). To further our analysis, we compared the Blimp-1–activated genes with our recently defined signature of 301 PC genes[6] and found that 88% (264/301) of the signature genes were expressed independently of Blimp-1 (Fig. 2e). When combined with previous studies[10-12,16,20,29], these results demonstrate that although Blimp-1 is essential for the establishment of the full PC gene expression program, once formed, PCs maintain their unique transcriptome largely independent of Blimp-1.

Blimp-1 controls plasma cell size and ultrastructure

During our analysis of the survival kinetics, we noticed that the Blimp-1–deleted PCs displayed a smaller size, granularity and a continuum of reduced expression of CD138 and Blimp-1-GFP (Fig. 3a). Transmission electron microscopic examination of the cellular ultrastructure also revealed that Blimp-1–deficient BM PCs displayed a severe disruption of their distinctive dense ER (Fig. 3b), a finding substantiated by staining by with a fluorescent dye specific for the ER (Fig. 3c). By contrast, staining for secretory granules, using lysotracker, was increased in Blimp-1–deficient PCs, suggesting impaired lysosomal

trafficking. As an independent measure of secretory activity of the PCs we measured the cell surface exposure of the lysosome-associated protein CD107a (Fig. 3c). Blimp-1–deficient BM PCs had strongly decreased CD107a staining, again indicative of impaired lysosomal fusion with the plasma membrane. Thus Blimp-1 is required to maintain the characteristic PC morphology and cytoplasmic organization.

Blimp-1 controls immunoglobulin secretion

As the fundamental function of PCs is to produce immunoglobulin, we assessed the secretory capacity of Blimp-1–sufficient and –deficient PCs by ELISPOT assay. Spleen and BM PCs were purified 14–28 days after tamoxifen treatment and tested for IgM and pan-IgG secretion (Fig. 4a). Secretion of both immunoglobulin isotypes was reduced in the spleen and, most strikingly, the BM in absence of Blimp-1. To determine if this defect resulted from a decrease in *Ig* transcription we examined our RNA sequencing data and found that, with the notable exception of those encoding IgM *(Ighm)* and IgG3 *(Ighg3)*, *Ig* transcripts were not affected by Blimp-1 loss (Fig. 4b).

The *Igh* isotypes are produced in two different isoforms that differ in their use of polyadenylation sites[32]. The longer membrane-bound receptor form is highly expressed in B cells, while the shorter secreted form predominates in PCs (Supplementary Fig. 3a). Closer inspection of the expression of the exon use of the *Igh* constant regions revealed a relative increase in the transmembrane form in Blimp-1–deficient PCs, thus lowering the ratio between secreted and membrane-bound transcripts (Fig. 4c,d). We then assessed the protein expression by intracellular flow cytometry staining. The proportion of IgG^+, IgA^+ or $Ig\kappa\lambda^+$ PCs was similar in Blimp-1–deficient and control PCs (Fig. 4e and data not shown). In line with the reduced *Ighm* expression, the frequency of IgM^+ PCs was severely diminished (Fig. 4e). Intra- and extracellular flow cytometry staining for IgA and IgM confirmed that whereas the total protein expression was decreased, the membrane-bound form was maintained (Fig. 4f). The elongation factor Ell2 has been shown to play a major role in this alternative polyadenylation process[33,34]. *Ell2* was a direct target of Blimp-1 (Supplementary Table 1) and its expression was reduced in Blimp-1–deficient PCs (Fig. 4g). Those data suggest that Blimp-1 contributes to the efficient transition from a membrane-bound to a secreted form of *Igh* in PCs, at least in part through the direct control of *Ell2* expression.

Blimp-1 regulates the unfolded protein response

The partial re-expression of the membrane-bound *Igh* at the expense of the secreted isoform could only partially explain the secretion defect observed after Blimp-1 inactivation. Therefore we examined the expression of the major regulators of the UPR that controls protein synthesis, folding, posttranslational modifications and expansion of the secretory apparatus (Supplementary Fig. 3b). Importantly, XBP-1, ATF4 and ATF6, the three main transcription factors known to implement this pathway,[4,35] were all significantly down-regulated at the mRNA and protein levels in BM PCs after *Prdm1* inactivation (Fig. 5a and Supplementary Table 2). ChIPseq assay of *in vitro* generated PBs identified Blimp-1 binding sites in *Atf6*, but not *Atf4* or *Xbp1* (Fig. 5b and data not shown). The regulation of *Xbp1* by Blimp-1 is likely two-pronged, with Blimp-1 activating *Atf6*, a known inducer of *Xbp1* (ref. 36), and also promoting formation of the active spliced form of XBP-1(s) through the direct

regulation of *Ern1*, encoding Ire1 (Fig. 5b)[37]. The requirement for Blimp-1 for full expression of the key regulators of the UPR translated into a down-modulation of the expression of the majority of genes encoding the downstream components of the pathway (Fig. 5c, Supplementary Table 2 and Supplementary Fig. 4a). Interestingly, the function of Blimp-1 in the UPR was much broader than the regulation of the key transcription factors, as Blimp-1 directly bound to 38% (45/119) of UPR genes expressed in PCs, representing all branches of the pathway (Supplementary Table 2). Taken together these data demonstrate that Blimp-1 is a central transcription factor of the UPR in PCs.

To examine the overlap between Blimp-1 and XBP-1 in controlling the UPR and the PC transcriptome more generally, we generated mice with inducible deletion of *Xbp1* using the Cre^{ERT2} system (Supplementary Fig. 2d). As previously reported, *Xbp1* inactivation had no impact on the size of the PC population[19,21,22] (Fig. 6a). RNA sequencing analysis revealed that 632 genes were differentially expressed in the absence of XBP-1 (Fig. 6b and Supplementary Table 3), and importantly *Prdm1* was not down-modulated, but mildly up-regulated without XBP-1 (fold change=1.68, FDR=0.047). The comparison of Blimp-1 and XBP-1–regulated genes showed only a modest overlap of 56 genes (31 activated, 25 inhibited, 12% of total), making it unlikely that the Blimp-1–mediated control of PC function was predominantly through XBP-1 regulation (Supplementary Fig. 4b), a conclusion that agrees with the earlier studies using *in vitro* derived PCs[20]. Of note, XBP-1-deficiency in BM PCs resulted in a global reduction in all *Igh* transcripts (Fig. 6c). Reduced immunoglobulin expression was confirmed at the protein level (Fig. 6d) and correlated with reduced secretory function, as measured by CD107a (Fig. 6e) and the size of ELISPOTs for IgA and IgM (Fig. 6f and data not shown). An overall analysis of the UPR pathway revealed a similar down-modulation (Fig. 6g) to that observed without Blimp-1 (Fig. 5c), however in contrast to Blimp-1, the activity of XBP-1 was focused on particular processes of the pathway, notably the protein folding and targeting to the ER, while having almost no effect on other effectors such as the transcription factors (Supplementary Table 2 and Supplementary Fig. 4a). XBP-1 loss also had very little impact on the expression of the B cell and PC signature genes, beyond the UPR (Supplementary Fig. 4c). This analysis reveals that while the functions of Blimp-1 and XBP-1 overlap in the control of *Igh* expression and some aspects of the UPR, most of their functions in PCs are unique.

Blimp-1 is required for full mTOR activity

A characteristic phenotype of the Blimp-1–deficient PCs was their decreased cell size, a feature that is under the control of the mTOR (mammalian target of rapamycin) pathway[38]. The kinase mTOR is part of two complexes, mTORC1 and mTORC2, the former regulating cell size, organelle biogenesis and proteosynthesis (Supplementary Fig. 3c). Analysis of the RNA sequencing data revealed that the expression of the core components of either complex, such as *Mtor, Raptor* and *Rictor,* was not affected by Blimp-1 loss in PCs (data not shown). In contrast, assessment of the activity of the mTORC1 complex through the phosphorylation of mTOR itself (Ser2448) and one of its downstream targets S6 (Ser235/236) revealed that the pathway activity was highly upregulated in PCs, compared to B cells, and dependent upon Blimp-1 (Fig. 7a). As a control, we tested the phosphorylation of an mTORC2 target, Akt (Ser473), and found it unaffected (Fig. 7a). Amino acid supply,

in particular leucine, is a crucial regulator of the mTORC1 activity[39], and we determined that the expression of several amino acid carriers was decreased in Blimp-1–deficient BM PCs (Fig. 7a,b). The expression of one of those carriers, CD98, was particularly high on PCs and strongly Blimp-1–dependent (Fig. 7a). CD98 is encoded by *Slc3a2* and *Slc7a5,* both Blimp-1–regulated genes, with the latter also being directly bound by Blimp-1 (Fig. 7b,c). The expression of the transferrin receptor (CD71, encoded by *Tfrc*), another carrier known to modulate mTORC1 activity, was also decreased in absence of Blimp-1 (Fig. 7b). Furthermore, two members of the Sestrin family[40], *Sesn1* and *Sesn3* were targets of Blimp-1–mediated repression, being bound by Blimp-1 and their expression was augmented in Blimp-1–deficient PCs (Fig. 7b,c). Sestrins are activators of the AMP-activated protein kinase (AMPK), which inhibits mTORC1 through the phosphorylation of one of its components, Raptor[41]. In keeping with increased AMPK activity, the phosphorylation of two AMPK targets, ACC (Acetyl-CoA carboxylase) (Ser79) and Raptor (Ser792), were significantly enhanced following loss of Blimp-1 (Fig. 7a). Those data suggested that Blimp-1 acts at multiple points to positively regulate mTORC1 activity; through the activation of the amino acid carrier, including CD98, and repression of the expression of the negative regulatory Sestrins, thus preventing AMPK activity.

DISCUSSION

IRF4, Blimp-1 and XBP-1 are the best characterized transcription factors active in mature PCs. By removing each one in fully differentiated PCs *in vivo*, our data demonstrated that these factors play specific roles in the PC biology. PC survival critically relied on IRF4, potentially through the regulation of a key survival molecule such as Mcl-1 (ref. 30). The ablation of the PC lineage at even early points after *Irf4*-inactivation agrees with previous studies using multiple myeloma cell lines[23] and precludes any further investigation into the IRF4 downstream targets using these *in vivo* models. By contrast, we determined that mature PCs survived the acute loss of either Blimp-1 or XBP-1. These findings contrast with earlier studies that concluded that both factors were essential for PC survival[18,28]. The major point of difference in these studies was that the previous authors predominantly tracked antibody abundance and specificity as a surrogate for PC frequency, thus the loss of antibody due to the greatly impaired secretion in both mutant mouse strains, gave the misleading impression of the disappearance of PCs. The use of the Blimp-1-GFP reporter also provided us with a superior tool to track the PCs at high resolution, compared to the use of CD138 or immunoglobulin secretion[11]. The survival of Blimp-1 and XBP-1 -deficient PCs is also compatible with the recent reports that both proteins may act as tumor suppressors in multiple myeloma[42,43].

Blimp-1 has long been known to be essential for the developmental transition between activated B cells and PCs[12]. Blimp-1 is thought to act by the repression of the major regulators of the B cell program, including *Pax5, Bcl6, Spib, Ciita*, as well as silencing *Myc* to facilitate the post-mitotic state of mature PCs (reviewed in[24]). By comparing our transcriptomic data with the recently reported PC signature[6] it was apparent that Blimp-1 was not required to maintain the core identity, as defined by their transcriptional program, of already mature PCs. Blimp-1 does play some role in repressing B cell transcription, as a number of B cell genes including those encoding CD23, CD22, Spi-B, Id3, and TLR9, but

not Pax-5, Bcl-6 or Myc were re-expressed without Blimp-1, suggesting that while some targets require active Blimp-1–mediated repression, the repression of others is maintained indirectly through other mechanisms in fully mature PCs. Our current findings, together with prior studies from a number of groups, suggest a model where Blimp-1 is essential for the establishment of the full plasma cell transcriptome[10-12,16,20,29], but once established plasma cell identity is maintained independent of Blimp-1.

Ig accounts for approximately 70% of total transcripts in long-lived PCs[6], allowing each cell to produce close to 2 ng of antibodies per day[44]. To reach and stably maintain this secretory capacity, PCs require specialized machinery and metabolic activity. Our data demonstrate that Blimp-1 plays a central role in this process through the enforcement of the UPR and mTOR pathways. In PCs, the UPR has been proposed to function not as a stress response, but as a preemptive physiological pathway, implemented during the early differentiation that precedes the high immunoglobulin expression[45]. Supporting this conclusion, we demonstrated that it is XBP-1, and not on the whole Blimp-1, that maintains the expression of *Ig* transcripts in mature PCs. Blimp-1 is intimately involved in the UPR, directly regulating *Atf6* and *Ern1*, both of whom are required for full XBP-1 expression and UPR function, as well as directly regulating 38% of the downstream genes in this pathway. Blimp-1 was also required to maintain the characteristic cytoplasmic morphology of PCs, a function also linked to the inability to fully activate XBP-1 (refs. 21,46).

Beyond the UPR the targets of Blimp-1 and XBP-1 were largely independent suggesting distinct functions in PC biology. The regulation of mTOR pathway activity by Blimp-1 represented one such unique role. mTOR has a complementary function to the UPR[47], as it modulates the proteosynthesis or the organelle biogenesis in response to environmental stimuli, and in particular to nutrient availability. Moreover, enhanced mTOR activity can promote immunoglobulin production independently of XBP-1 (ref. 46). Our data showed that Blimp-1 directly fostered this pathway through two independent mechanisms. Blimp-1 supported the amino acid supply of the PCs by directly promoting the expression of specific carriers, such as CD98, and prevented the activity of the inhibitory Sestrin–AMPK axis. Taken together our studies demonstrate that while the survival and identity of long-lived PCs is largely independent of Blimp-1, this multifunctional transcriptional regulator is essential for the molecular and cellular changes that support the extremely high and sustained rates of antibody secretion that are essential for protective immunity.

METHODS

Mice

Prdm1$^{gfp/+}$ [11], *Prdm1*^{fl} [25], *Irf4*^{fl} [26], *Xbp1*^{fl} [22] and *Rosa26*-Cre^{ERT2} [27] mice were bred and maintained at the animal facilities of the Walter and Eliza Hall Institute. *Prdm1*^{fl} mice carried a *lox*P-flanked exon 5, while *Prdm1*^{gfp} mice expressed an allele truncated after exon 5 (of a total of 7 exons). The PCR analysis for exon 5 loss has been described previously[25]. All mice were on C57BL/6 background. Animal experiments were conducted according to the protocols approved by the Walter and Eliza Hall Institute ethics committee. Immunization was a single intraperitoneal injection of 100 μg NP-KLH precipitated onto alum (ThermoScientific). For cell transfer experiments, total splenocytes (5×10^6) or

isolated B cells (2×10^6) were injected intravenously into *Rag1*$^{-/-}$ recipients. Cre-mediated deletion of *lox*P-flanked alleles was triggered by the administration of tamoxifen (Sigma-Aldrich, 0.2 mg/g) by oral gavage on two consecutive days.

Plasmablast generation *in vitro*

B cells were isolated from splenocytes by positive selection using the B220- or CD19-coated beads (Miltenyi Biotec) and cultured as previously described[48]. Cultures were seeded at 1×10^6/ml with optimal concentrations of CD40L (100 ng/ml; R&D Systems), IL-4 (10 ng/ml; R&D Systems) and IL-5 (5 ng/ml; R&D Systems). Cultures were treated with 4-hydroxytamoxifen (Sigma-Aldrich) at 100 nM.

Flow cytometry and cell sorting

Single-cell suspensions were stained with the following antibodies to surface molecules: CD138 (281.2; BD Biosciences), CD19 (1D3; in-house), B220 (RA3-6B2; in-house), IgM (II41; eBiosciences), CD98 (RL388; Biolegend), CD93 (AA4.1; BD Biosciences), MHCII (M5; eBiosciences), CD22 (OX-97; Biolegend), CD107a (1D4B; BD Biosciences), CD71 (B2; BD Biosciences). Cells were stained with lysotracker deep red or ERtracker red (Molecular Probes) according to manufacturer's instructions. For intracellular transcription factor and immunoglobulin measurement, cells were fixed and permeabilized using the eBiosciences transcription factor staining buffer set and BD Cytofix/Cytoperm kit respectively, then stained antibodies specific for: XBP-1s (Q3-695; BD Biosciences), ATF4 (D4B8; Cell Signaling), ATF6 (polyclonal; Abcam), IgM (polyclonal; Jackson Immunoresearch), IgG (polyclonal; Jackson Immunoresearch), IgA (mA-6E1; eBiosciences), Igκ (187.1; BD Biosciences), Igλ (TB28-2; BD biosciences). For phospho-protein detection, cells were prepared using BD Phosphoflow lyse/fix buffer and perm buffer III, and labeled with specific antibodies that recognize: p-S235/236-S6 (D57.2.25; Cell Signaling), p-S2448-mTOR (D9C2; Cell Signaling), p-S79-ACC (D7D11; Cell Signaling), p-S792-Raptor (polyclonal: Cell Signaling), p-S473-Akt (M89-61, BD biosciences). Stained cells were analyzed on a FACSCantoII or Fortessa X20 (BD Biosciences). PCs were enriched from BM cells with biotinylated anti-CD138 (8B12; in-house) and anti-biotin microbeads (Miltenyi Biotec) and sorted with FACSDiva or Aria cytometers (BD Biosciences).

ELISPOT assay

Multiscreen-HA plates (Millipore) were coated with anti-mouse Immunoglobulin. Cells were incubated on the plates overnight at 37 °C. After incubation with biotinylated antibodies, followed by streptavidin-alkaline phosphatase, spots were developed using the substrate VectorBlue (Vector Labs). All antibodies used for coating and labeling were obtained from Southern Biotechnology Inc.

Whole transcriptome analysis

RNA was isolated from *ex vivo* sorted Blimp-1-GFP$^+$CD138$^+$ PCs from previously tamoxifen treated *Prdm1*$^{+/gfp}$Cre^{ERT2}, *Prdm1*$^{fl/gfp}$Cre^{ERT2}, *Xbp1*$^{fl/fl}$ *Prdm1*$^{+/gfp}$Cre^{ERT2} and *Xbp1*$^{+/+}$ *Prdm1*$^{+/gfp}$Cre^{ERT2} BM using the Qiagen RNeasy Micro kit. Libraries were

generated using the Illumina Truseq RNA sample preparation kit following manufacturer instructions. Two biological replicates, each containing material pooled from multiple individual mice, were generated and sequenced for each sample. For all samples 100 ng RNA were subjected to a transcriptome 75–100 bp single-end sequencing on an Illumina HiSeq 2500 instrument at the Australian Genome Research Facility. Raw RNA-seq data previously generated for follicular B cells (GSE60927) were also included in this analysis.

Sequence reads were aligned to the GRCm38/mm10 build of the *Mus musculus* genome using the Subread aligner[49]. Only uniquely mapped reads were retained. Genewise counts were obtained using featureCounts[50]. Reads overlapping exons in annotation build 38.1 of NCBI RefSeq database were included. *Ig* genes were excluded from the gene-level expression analysis and were analyzed separately. Genes were filtered from downstream analysis if they failed to achieve a c.p.m. (counts per million mapped reads) value of at least 1 in at least one library. Counts were converted to log2 counts per million, quantile normalized and precision weighted with the 'voom' function of the limma package[51,52]. A linear model was fitted to each gene, and empirical Bayes moderated *t*-statistics were used to assess differences in expression[53]. Genes were called differentially expressed if they achieved a FDR of 0.05 or less. The gene set enrichment plots were generated with the 'barcodeplot' function in limma. Gene set enrichment analysis was carried out using the 'roast' method in limma with 999 rotations[54]. One-sided *P* values are reported.

For the analysis of *Ig* genes, sequence reads were re-aligned to the genome using the Subjunc aligner with the "--allJunctions" option to disable the requirement for the presence of donor and receptor sites when mapping exon-spanning reads[49]. Mapped reads were then assigned to all exons using featureCounts. Exon-spanning reads were assigned to all their overlapping exons. RPKM (reads per kilobase of exon length per million mapped fragments) values for *Ig* constant exons were computed based on exon lengths and the total exon counts in each library. The Subjunc mapping data were also used to identify the frequency of splicing between *Prdm1* exons 5–6 and 4–6 and thus the efficiency of Cre-mediated deletion of the *lox*P-flanked exon 5 in PCs.

Transmission electron microscopy

BM Blimp-1-GFP^{+}CD138^{+} PCs were purified by flow cytometry and prepared for transmission electron microscopy as previously described[21].

Bio-ChIP-seq analysis of Blimp-1 binding

CD138^{+} PBs were generated by LPS-induced differentiation of mature B cells from *Prdm1*$^{Bio/Bio}$*Rosa26*$^{BirA/BirA}$ mice as described in detail elsewhere[29]. Chromatin from ~1 × 10^{8} PBs was prepared using a lysis buffer containing 0.25% SDS prior to chromatin precipitation by streptavidin pulldown (Bio-ChIP), as described[55]. The precipitated genomic DNA was quantified by real-time PCR, and about 1–5 ng of ChIP-precipitated DNA was used for library preparation and subsequent Illumina deep sequencing. Peak calling and gene assignment is described in detail elsewhere[29].

Supplementary Material

Refer to Web version on PubMed Central for supplementary material.

ACKNOWLEDGEMENTS

We are grateful to U. Klein (Columbia University, New York) and L. Glimcher (Weill Cornell Medical College, New York) for mice, S. Wilcox, M. Chopin and C. Seillet for technical assistance and J. Leahy for animal care. This work was supported by the National Health and Medical Research Council of Australia (IRIISS grant #361646, Program Grants #575500 and 1054925 to S.L.N., Program Grant #1054618 to G.K.S., Project Grant #1023454 to G.K.S. and W.S., Project Grant #1049416 to A.K. and fellowships to G.K.S. and S.L.N.), a fellowship from the Sylvia and Charles Viertel Foundation (to A.K.) and a research grant from the Multiple Myeloma Research Foundation (MMRF, to S.L.N). Research in the Busslinger laboratory was supported by Boehringer Ingelheim and an ERC Advanced Grant (291740-LymphoControl). This work was made possible through Victorian State Government Operational Infrastructure Support.

REFERENCES

1. Tarlinton D, Radbruch A, Hiepe F, Dorner T. Plasma cell differentiation and survival. Curr Opin Immunol. 2008; 20:162–169. [PubMed: 18456483]
2. MacLennan IC, et al. Extrafollicular antibody responses. Immunol Rev. 2003; 194:8–18. [PubMed: 12846803]
3. Hammarlund E, et al. Duration of antiviral immunity after smallpox vaccination. Nat Med. 2003; 9:1131–1137. [PubMed: 12925846]
4. Bettigole SE, Glimcher LH. Endoplasmic reticulum stress in immunity. Annu Rev Immunol. 2015; 33:107–138. [PubMed: 25493331]
5. Nutt SL, Hodgkin PD, Tarlinton DM, Corcoran LM. The generation of antibody-secreting plasma cells. Nat Rev Immunol. 2015; 15:160–171. [PubMed: 25698678]
6. Shi W, et al. Transcriptional profiling of mouse B cell terminal differentiation defines a signature for antibody-secreting plasma cells. Nat Immunol. 2015; 16:663–673. [PubMed: 25894659]
7. Kwon H, et al. Analysis of IL-21-induced Prdm1 gene regulation reveals functional cooperation of STAT3 and IRF4 transcription factors. Immunity. 2009; 31:941–952. [PubMed: 20064451]
8. Ochiai K, et al. Transcriptional regulation of germinal center B and plasma cell fates by dynamical control of IRF4. Immunity. 2013; 38:918–929. [PubMed: 23684984]
9. Sciammas R, et al. Graded expression of interferon regulatory factor-4 coordinates isotype switching with plasma cell differentiation. Immunity. 2006; 25:225–236. [PubMed: 16919487]
10. Kallies A, et al. Initiation of plasma-cell differentiation is independent of the transcription factor Blimp-1. Immunity. 2007; 26:555–566. [PubMed: 17509907]
11. Kallies A, et al. Plasma cell ontogeny defined by quantitative changes in blimp-1 expression. J Exp Med. 2004; 200:967–977. [PubMed: 15492122]
12. Shapiro-Shelef M, et al. Blimp-1 is required for the formation of immunoglobulin secreting plasma cells and pre-plasma memory B cells. Immunity. 2003; 19:607–620. [PubMed: 14563324]
13. Lin KI, Angelin-Duclos C, Kuo TC, Calame K. Blimp-1-dependent repression of Pax-5 is required for differentiation of B cells to immunoglobulin M-secreting plasma cells. Mol Cell Biol. 2002; 22:4771–4780. [PubMed: 12052884]
14. Lin Y, Wong K, Calame K. Repression of c-myc transcription by Blimp-1, an inducer of terminal B cell differentiation. Science. 1997; 276:596–609. [PubMed: 9110979]
15. Piskurich JF, et al. BLIMP-I mediates extinction of major histocompatibility class II transactivator expression in plasma cells. Nat Immunol. 2000; 1:526–532. [PubMed: 11101876]
16. Shaffer AL, et al. Blimp-1 orchestrates plasma cell differentiation by extinguishing the mature B cell gene expression program. Immunity. 2002; 17:51–62. [PubMed: 12150891]
17. Doody GM, et al. An extended set of PRDM1/BLIMP1 target genes links binding motif type to dynamic repression. Nucleic Acids Res. 2010; 38:5336–5350. [PubMed: 20421211]

18. Reimold AM, et al. Plasma cell differentiation requires the transcription factor XBP-1. Nature. 2001; 412:300–307. [PubMed: 11460154]
19. Hu CC, Dougan SK, McGehee AM, Love JC, Ploegh HL. XBP-1 regulates signal transduction, transcription factors and bone marrow colonization in B cells. EMBO J. 2009; 28:1624–1636. [PubMed: 19407814]
20. Shaffer AL, et al. XBP1, downstream of Blimp-1, expands the secretory apparatus and other organelles, and increases protein synthesis in plasma cell differentiation. Immunity. 2004; 21:81–93. [PubMed: 15345222]
21. Taubenheim N, et al. High Rate of Antibody Secretion Is not Integral to Plasma Cell Differentiation as Revealed by XBP-1 Deficiency. J Immunol. 2012; 189:3328–3338. [PubMed: 22925926]
22. Todd DJ, et al. XBP1 governs late events in plasma cell differentiation and is not required for antigen-specific memory B cell development. J Exp Med. 2009; 206:2151–2159. [PubMed: 19752183]
23. Shaffer AL, et al. IRF4 addiction in multiple myeloma. Nature. 2008; 454:226–231. [PubMed: 18568025]
24. Shapiro-Shelef M, Calame K. Regulation of plasma-cell development. Nat. Rev. Immunol. 2005; 5:230–242. [PubMed: 15738953]
25. Kallies A, Xin A, Belz GT, Nutt SL. Blimp-1 transcription factor is required for the differentiation of effector CD8(+) T cells and memory responses. Immunity. 2009; 31:283–295. [PubMed: 19664942]
26. Klein U, et al. Transcription factor IRF4 controls plasma cell differentiation and class-switch recombination. Nat Immunol. 2006; 7:773–782. [PubMed: 16767092]
27. Seibler J, et al. Rapid generation of inducible mouse mutants. Nucleic Acids Res. 2003; 31:e12. [PubMed: 12582257]
28. Shapiro-Shelef M, Lin KI, Savitsky D, Liao J, Calame K. Blimp-1 is required for maintenance of long-lived plasma cells in the bone marrow. J Exp Med. 2005; 202:1471–1476. [PubMed: 16314438]
29. Minnich M, et al. Multifunctional role of the transcription factor Blimp1 in coordinating plasma cell differentiation. Nat Immunol. 2015 in press.
30. Peperzak V, et al. Mcl-1 is essential for the survival of plasma cells. Nat Immunol. 2013; 14:290–297. [PubMed: 23377201]
31. O'Connor BP, et al. BCMA is essential for the survival of long-lived bone marrow plasma cells. J Exp Med. 2004; 199:91–98. [PubMed: 14707116]
32. Bayles I, Milcarek C. Plasma cell formation, secretion, and persistence: the short and the long of it. Crit Rev Immunol. 2014; 34:481–499. [PubMed: 25597311]
33. Martincic K, Alkan SA, Cheatle A, Borghesi L, Milcarek C. Transcription elongation factor ELL2 directs immunoglobulin secretion in plasma cells by stimulating altered RNA processing. Nat Immunol. 2009; 10:1102–1119. [PubMed: 19749764]
34. Park KS, et al. Transcription elongation factor ELL2 drives Ig secretory-specific mRNA production and the unfolded protein response. J Immunol. 2014; 193:4663–4674. [PubMed: 25238757]
35. Brewer JW. Regulatory crosstalk within the mammalian unfolded protein response. Cell Mol Life Sci. 2014; 71:1067–1079. [PubMed: 24135849]
36. Yoshida H, Matsui T, Yamamoto A, Okada T, Mori K. XBP1 mRNA is induced by ATF6 and spliced by IRE1 in response to ER stress to produce a highly active transcription factor. Cell. 2001; 107:881–891. [PubMed: 11779464]
37. Calfon M, et al. IRE1 couples endoplasmic reticulum load to secretory capacity by processing the XBP-1 mRNA. Nature. 2002; 415:92–96. [PubMed: 11780124]
38. Powell JD, Pollizzi KN, Heikamp EB, Horton MR. Regulation of immune responses by mTOR. Annu Rev Immunol. 2012; 30:39–68. [PubMed: 22136167]
39. Edinger AL, Thompson CB. Akt maintains cell size and survival by increasing mTOR-dependent nutrient uptake. Mol Biol Cell. 2002; 13:2276–2288. [PubMed: 12134068]

40. Lee JH, Budanov AV, Karin M. Sestrins orchestrate cellular metabolism to attenuate aging. Cell Metab. 2013; 18:792–801. [PubMed: 24055102]
41. Chen CC, et al. FoxOs inhibit mTORC1 and activate Akt by inducing the expression of Sestrin3 and Rictor. Dev Cell. 2010; 18:592–604. [PubMed: 20412774]
42. Leung-Hagesteijn C, et al. Xbp1s-negative tumor B cells and pre-plasmablasts mediate therapeutic proteasome inhibitor resistance in multiple myeloma. Cancer Cell. 2013; 24:289–304. [PubMed: 24029229]
43. Lohr JG, et al. Widespread genetic heterogeneity in multiple myeloma: implications for targeted therapy. Cancer Cell. 2014; 25:91–101. [PubMed: 24434212]
44. Brinkmann V, Heusser CH. T cell-dependent differentiation of human B cells into IgM, IgG, IgA, or IgE plasma cells: high rate of antibody production by IgE plasma cells, but limited clonal expansion of IgE precursors. Cell Immunol. 1993; 152:323–332. [PubMed: 8258141]
45. Gass JN, Gifford NM, Brewer JW. Activation of an unfolded protein response during differentiation of antibody-secreting B cells. J Biol Chem. 2002; 277:49047–49054. [PubMed: 12374812]
46. Benhamron S, Pattanayak SP, Berger M, Tirosh B. mTOR activation promotes plasma cell differentiation and bypasses XBP-1 for immunoglobulin secretion. Mol Cell Biol. 2015; 35:153–166. [PubMed: 25332234]
47. Goldfinger M, Shmuel M, Benhamron S, Tirosh B. Protein synthesis in plasma cells is regulated by crosstalk between endoplasmic reticulum stress and mTOR signaling. Eur J Immunol. 2011; 41:491–502. [PubMed: 21268018]
48. Hasbold J, Corcoran LM, Tarlinton DM, Tangye SG, Hodgkin PD. Evidence from the generation of immunoglobulin G-secreting cells that stochastic mechanisms regulate lymphocyte differentiation. Nat Immunol. 2004; 5:55–63. [PubMed: 14647274]
49. Liao Y, Smyth GK, Shi W. The Subread aligner: fast, accurate and scalable read mapping by seed-and-vote. Nucleic Acids Res. 2013; 41:e108. [PubMed: 23558742]
50. Liao Y, Smyth GK, Shi W. featureCounts: an efficient general purpose program for assigning sequence reads to genomic features. Bioinformatics. 2014; 30:923–930. [PubMed: 24227677]
51. Law CW, Chen Y, Shi W, Smyth GK. voom: Precision weights unlock linear model analysis tools for RNA-seq read counts. Genome Biol. 2014; 15:R29. [PubMed: 24485249]
52. Ritchie ME, et al. limma powers differential expression analyses for RNA-sequencing and microarray studies. Nucleic Acids Res. 2015; 43:e47. [PubMed: 25605792]
53. Smyth GK. Linear models and empirical bayes methods for assessing differential expression in microarray experiments. Stat Appl Genet Mol Biol. 2004; 3 Article3.
54. Wu D, et al. ROAST: rotation gene set tests for complex microarray experiments. Bioinformatics. 2010; 26:2176–2182. [PubMed: 20610611]
55. Ebert A, et al. The distal V(H) gene cluster of the Igh locus contains distinct regulatory elements with Pax5 transcription factor-dependent activity in pro-B cells. Immunity. 2011; 34:175–187. [PubMed: 21349430]

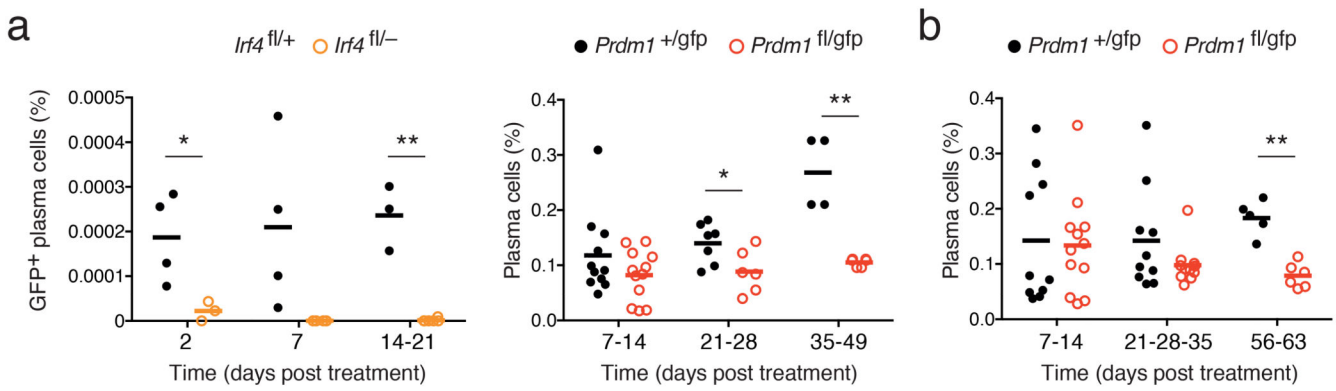

Figure 1.

Inactivation of *Irf4* and *Prdm1* in plasma cells. **(a)** *Rag1*$^{-/-}$ mice transferred with conditional knockout or control B cells were treated with tamoxifen to induce Cre activity and analyzed at the indicated time points, using the experimental plan outlined in Supplementary Fig. 1a. Left, frequency of *Irf4*$^{fl/+}$Cre^{ERT2} or *Irf4*$^{fl/-}$Cre^{ERT2} GFP^{+} PCs (out of total BM cells) was determined at the indicated day after tamoxifen treatment to induce *Irf4* inactivation (reported by GFP expression). PCs were identified as CD138^{+}B220^{lo}. Right, frequency of *Prdm1*$^{+/gfp}$Cre^{ERT2} (+/gfp) or *Prdm1*$^{fl/gfp}$Cre^{ERT2} (fl/gfp) BM PCs at the indicated day after tamoxifen treatment. PCs were identified as CD138^{+}Blimp-1-GFP^{+}. **(b)** Frequency of BM PCs from intact *Prdm1*$^{+/gfp}$Cre^{ERT2} or *Prdm1*$^{fl/gfp}$Cre^{ERT2} mice at the indicated day after tamoxifen treatment, using the experimental plan outlined in Supplementary Fig. 1b. Each symbol in **a**,**b** represent data from a single mouse. Mean value is shown by a horizontal line. *P* values compare the indicated groups using a paired *t*-test. * *P*<0.05, ** P<0.005.

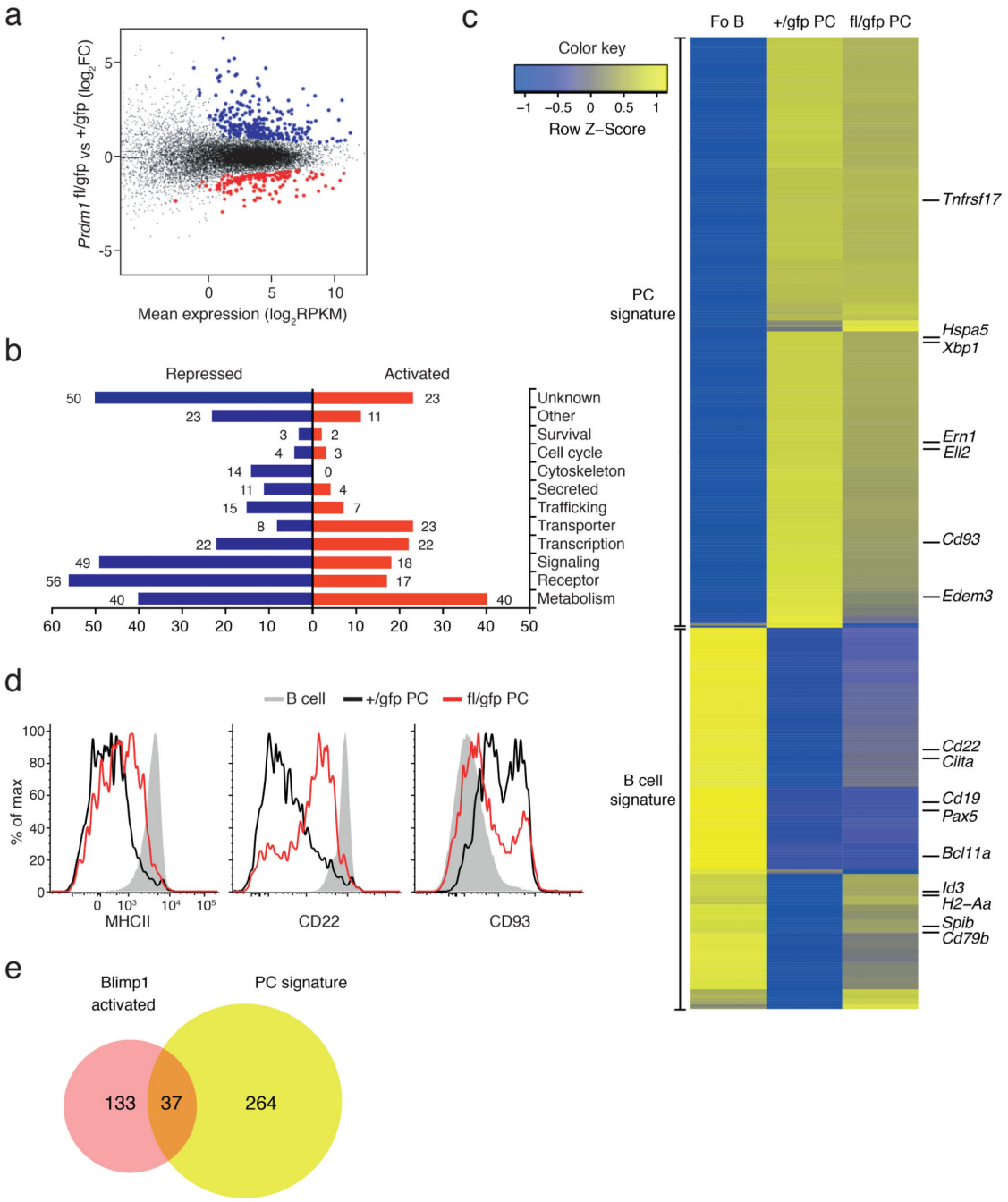

Figure 2.

Transcriptional analysis of Blimp-1-deficient plasma cells. **(a–c)** Whole genome RNA-sequencing analysis on BM PCs, sorted from *Prdm1*$^{+/gfp}$Cre^{ERT2} (+/gfp) or *Prdm1*$^{fl/gfp}$Cre^{ERT2} (fl/gfp) mice 21 days after tamoxifen treatment. **(a)** Scatter plot of differential expression. Genes with significantly increased (Blimp-1-repressed, blue) or decreased (Blimp-1-activated, red) expression in the absence of Blimp-1 (fl/gfp) are indicated (FDR <0.05, normalized average expression ≥4 RPKM in at least one sample). **(b)** Functional classification and quantification of proteins encoded by repressed (blue) and

activated (red) Blimp-1 targets in PCs. **(c)** Heat map shows the expression of the published gene signatures for follicular B cells (Fo B)[6] and BM PCs[6] from +/gfp and fl/gfp mice. The positions of some genes of interest are highlighted. **(d)** Flow cytometry profiles of BM mature B cells ($B220^{hi}CD19^{hi}$) and PCs ($CD138^{+}$Blimp-1-GFP^{+}) showing Blimp-1–regulated surface molecules after 21 days after tamoxifen treatment. Data is representative of at least 3 experiments. **(e)** Venn diagram showing overlap and differences between Blimp-1 activated target genes (Supplementary Table 1) and the PC gene signature[6]. Data in **a–c, e** derive from 2 experiments.

Europe PMC Funders Author Manuscripts

Europe PMC Funders Author Manuscripts

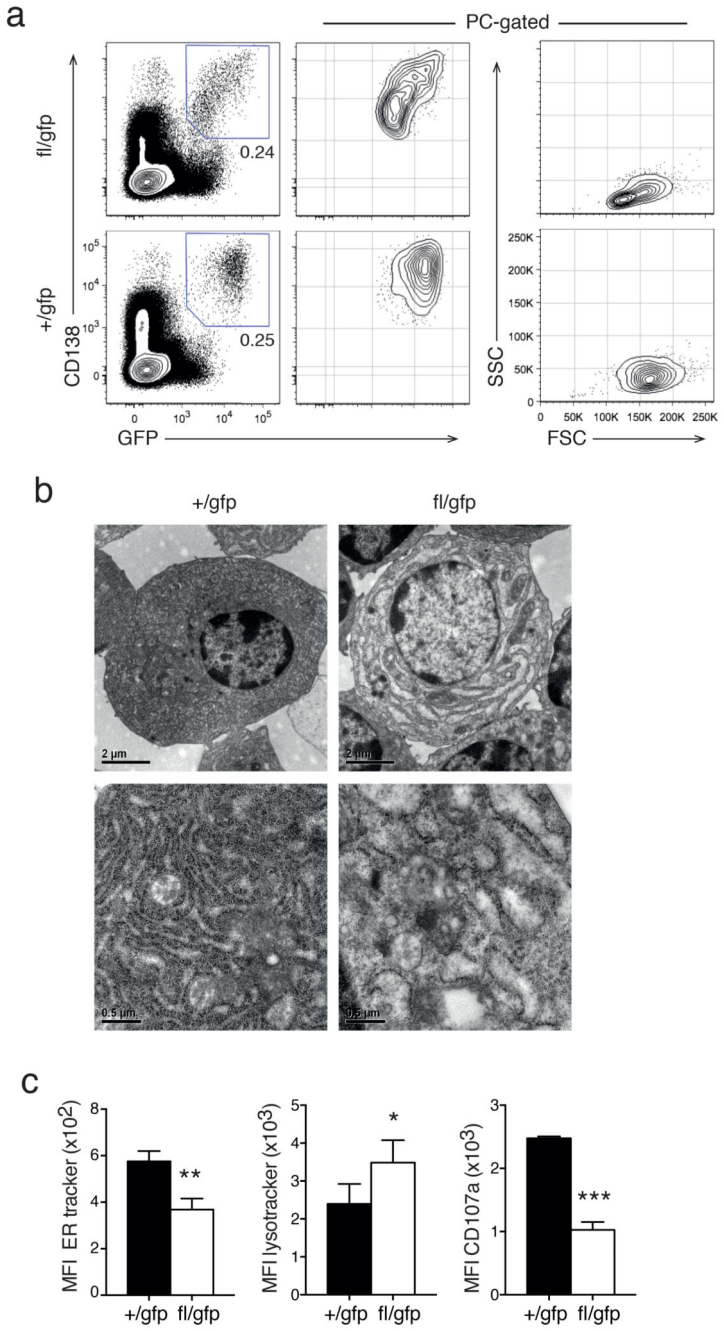

Figure 3.

Blimp-1 controls plasma cell size and morphology. **(a)** Cytometry profiles of *Prdm1*$^{+/gfp}$Cre^{ERT2} (+/gfp) and *Prdm1*$^{fl/gfp}$Cre^{ERT2} (fl/gfp) BM cells (left) and gated CD138^{+}Blimp-1-GFP^{+} PCs (middle and right) 35 days after tamoxifen treatment. Data is representative of 5 experiments. **(b)** Electron micrograph of isolated +/gfp and fl/gfp BM PCs 21 days after tamoxifen treatment. Data is representative of 2 experiments. **(c)** Mean fluorescent index (MFI) of organelle specific dyes (left, ER mitotracker and middle, lysotracker) and of surface CD107a expression (right) of +/gfp and fl/gfp BM cells 35 days

after tamoxifen treatment. Data is the mean ± S.D. from 3 experiments. *P* values compare the indicated groups using a paired t-test. * $P<0.05$, ** $P<0.01$, *** $P<0.005$.

Europe PMC Funders Author Manuscripts

Europe PMC Funders Author Manuscripts

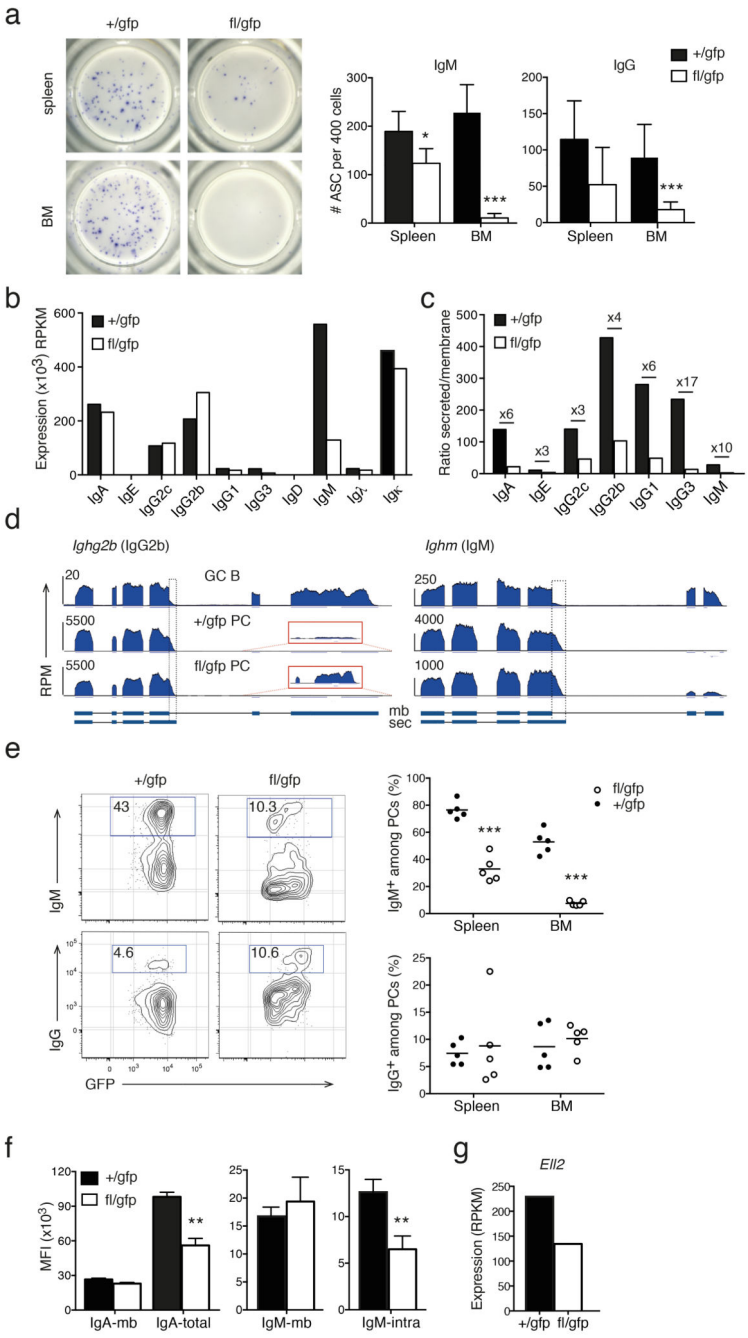

Figure 4.

Blimp-1 controls immunoglobulin production. **(a)** ELISPOT assay for IgM and pan-IgG secretion from isolated +/gfp and fl/gfp PCs 14 days after tamoxifen treatment. Left, images of representative wells of an anti-IgM assay. Right, graphs depict mean ± S.D. from a representative of 2 experiments. **(b-d)** RNA sequencing analysis of *Igh* transcripts in +/gfp and fl/gfp BM PCs analyzed as described in Fig. 2. **(b)** Normalized expression in RPKM of *Igh* and *Igl* constant regions. **(c)** Ratio of secreted (sec) / membrane-bound (mb) mRNA for each *Igh* isotype. Numbers specify the fold change between +/gfp and fl/gfp cells. **(d)** RNA

sequencing tracks of *Ighg2b* and *Ighm* in *Prdm1*$^{+/gfp}$ GC B cells, +/gfp and fl/gfp BM PCs. Boxes with dotted lines delineates the secretion specific sequences. Red boxes show the increased usage of the membrane specific exons of *Ighg2b* (magnified 85×). **(e)** Cytometry profiles of +/gfp and fl/gfp BM PCs 28 days after tamoxifen treatment showing intracellular staining of IgM and IgG (left). Right, graphs depict the percentage of IgM$^+$ or IgG$^+$ cells among the Blimp-1-GFP$^+$ PC population in spleen and BM. Symbols show individual mice, horizontal line is the mean. **(f)** Left, mean fluorescence index (MFI) of plasma membrane (mb) or total (mb and intracellular) expression of IgA, detected by sequential staining with the same Ab, in +/gfp and fl/gfp BM PCs 35 days after tamoxifen treatment. Right, MFI of plasma membrane (mb) or specific intracellular (intra) expression of IgM, detected by separate anti-IgM Abs, in +/gfp and fl/gfp BM PCs 35 days after tamoxifen treatment. Graphs depict mean ± S.D. from ≥2 experiments. **(g)** RNA sequencing analysis of the expression of *Ell2* in +/gfp and fl/gfp BM PCs as described in Fig. 2. *P* values compare the indicated groups using a paired *t*-test. * $P<0.05$, ** $P<0.01$, *** $P<0.005$.

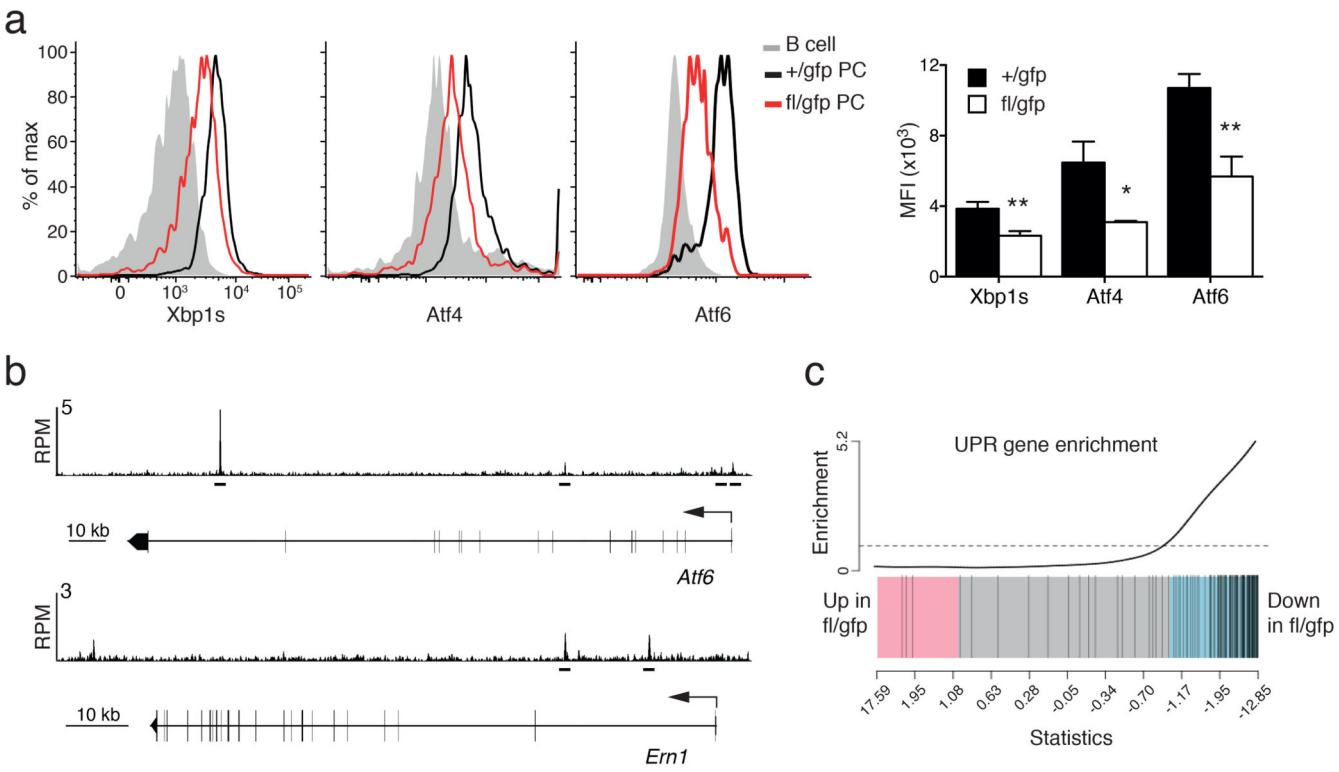

Figure 5.

Blimp-1 controls the unfolded protein response (UPR). **(a)** Cytometry profiles of intracellular staining of the expression of the key transcription factors of the UPR pathway: XBP-1s, Atf4 and Atf6, in *Prdm1*$^{+/gfp}$Cre^{ERT2} (+/gfp) and *Prdm1*$^{fl/gfp}$Cre^{ERT2} (fl/gfp) BM PCs 35 days after tamoxifen treatment. Graph shows the mean fluorescent index (MFI) of expression in PCs from ≥2 experiments. *P* values compare the indicated groups using a paired *t*-test. * $P < 0.05$, ** $P < 0.01$. **(b)** Blimp-1 binding at the *Atf6* and *Ern1* (encodes for Ire1) genes in LPS stimulated *Prdm1*$^{Bio/Bio}$*Rosa26*$^{BirA/BirA}$ tagged PBs. Blimp-1 peaks are shown together with the exon-intron structure of the gene and a scale bar in kilobases (kb). RPM, reads per million reads. Bars below the tracks indicate Blimp-1-binding regions identified by MACS peak calling. **(c)** Gene set enrichment analysis barcode plot comparing differential gene expression in fl/gfp and +/gfp BM PCs after tamoxifen treatment, as in Fig. 2. The differential gene expression dataset is shown as a shaded rectangle with genes horizontally ranked by moderated t statistic. Genes upregulated upon Blimp-1 loss shaded pink ($t > 1$) and downregulated genes shaded blue ($t < -1$). The 119 UPR genes, identified by gene annotation and filtered for expression in PCs, are marked on the plot by vertical black lines and enriched for genes downregulated without Blimp-1 ($P = 0.001$).

Europe PMC Funders Author Manuscripts

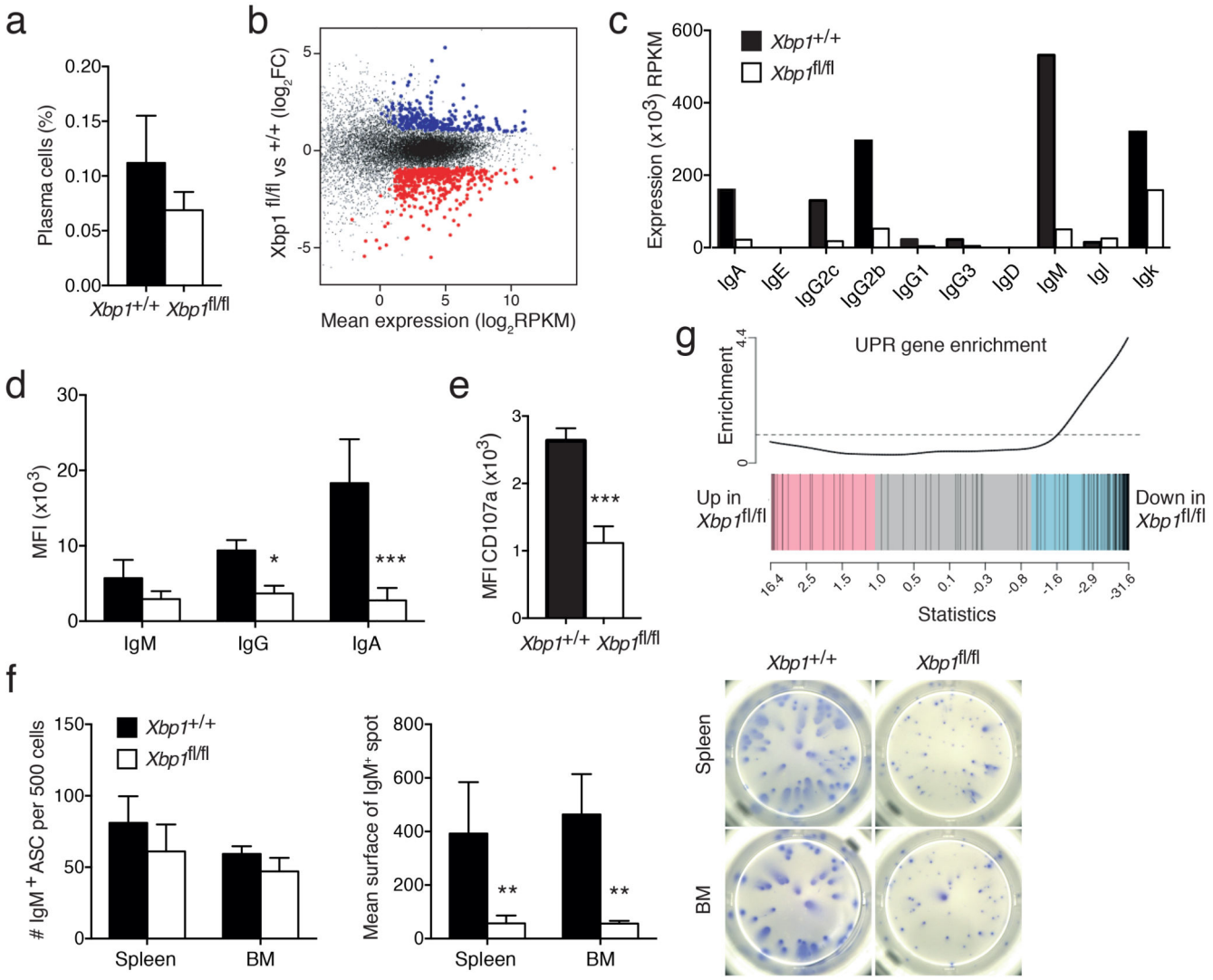

Figure 6.

XBP-1 loss leads to reduced *Igh* expression and unfolded protein response (UPR) activity. **(a-g)** *Xbp1*$^{+/+}$ *Prdm1*$^{+/gfp}$Cre^{ERT2} (+/+) or *Xbp1*$^{fl/fl}$ *Prdm1*$^{+/gfp}$Cre^{ERT2} (fl/fl) mice were treated with tamoxifen to induce XBP-1 inactivation. PCs were identified as CD138^{+}Blimp-1-GFP^{+} cells, 21 (**b-d**, **f-g**) or 35 (**a**, **e**) days later. **(a)** The proportion of BM PCs in a representative experiment. Graphs depict mean ± S.D. from 1 of 2 experiments. **(b)** Scatter plot of differential expression. Genes with significantly increased (XBP-1-repressed, blue) or decreased (XBP-1-activated, red) expression in the absence of XBP-1 (fl/fl) are indicated (FDR <0.05, normalized average expression ≥4 RPKM in at least one sample). **(c)** Normalized expression of the constant exons of the *Igh* and *Igl* chain genes in +/+ or fl/fl BM PCs. **(d)** Intracellular staining for Ig isotypes in +/+ or fl/fl BM PCs. Mean fluorescence index (MFI) for IgM, IgA and IgG was measured on IgA^{-}IgG^{-}, IgM^{-}IgG^{-} and IgA^{-}IgM^{-} cells, respectively. Graphs depict mean ± S.D. from 2 experiments. **(e)** MFI of CD107a expression at the surface of +/+ or fl/fl BM PCs. Graphs depict mean ± S.D. from 2 experiments. **(f)** ELISPOT assay for IgM secretion by isolated +/+ or fl/fl PCs. Left, Graphs

depict mean number of IgM^+ cells ± S.D. per 500 sorted Blimp-1-GFP^+CD138^+ PCs from 1 of 2 experiments. Middle, mean surface area ± S.D. of the spots identified. Right, pictures show representative wells of an anti-IgM assay. **(g)** Gene set enrichment plot for the UPR gene expression in +/+ or fl/fl BM PCs after tamoxifen treatment. The differential gene expression dataset is shown as a shaded rectangle with genes horizontally ranked by moderated *t* statistic. Genes upregulated upon XBP-1 loss shaded pink ($t > 1$) and downregulated genes shaded blue ($t < -1$). The 119 UPR genes, identified on the plot by black vertical lines, are enriched for genes downregulated without XBP-1 ($P=0.0005$). *P* values compare the indicated groups using a paired *t*-test. * $P < 0.05$, ** $P < 0.01$, *** $P < 0.005$.

Europe PMC Funders Author Manuscripts

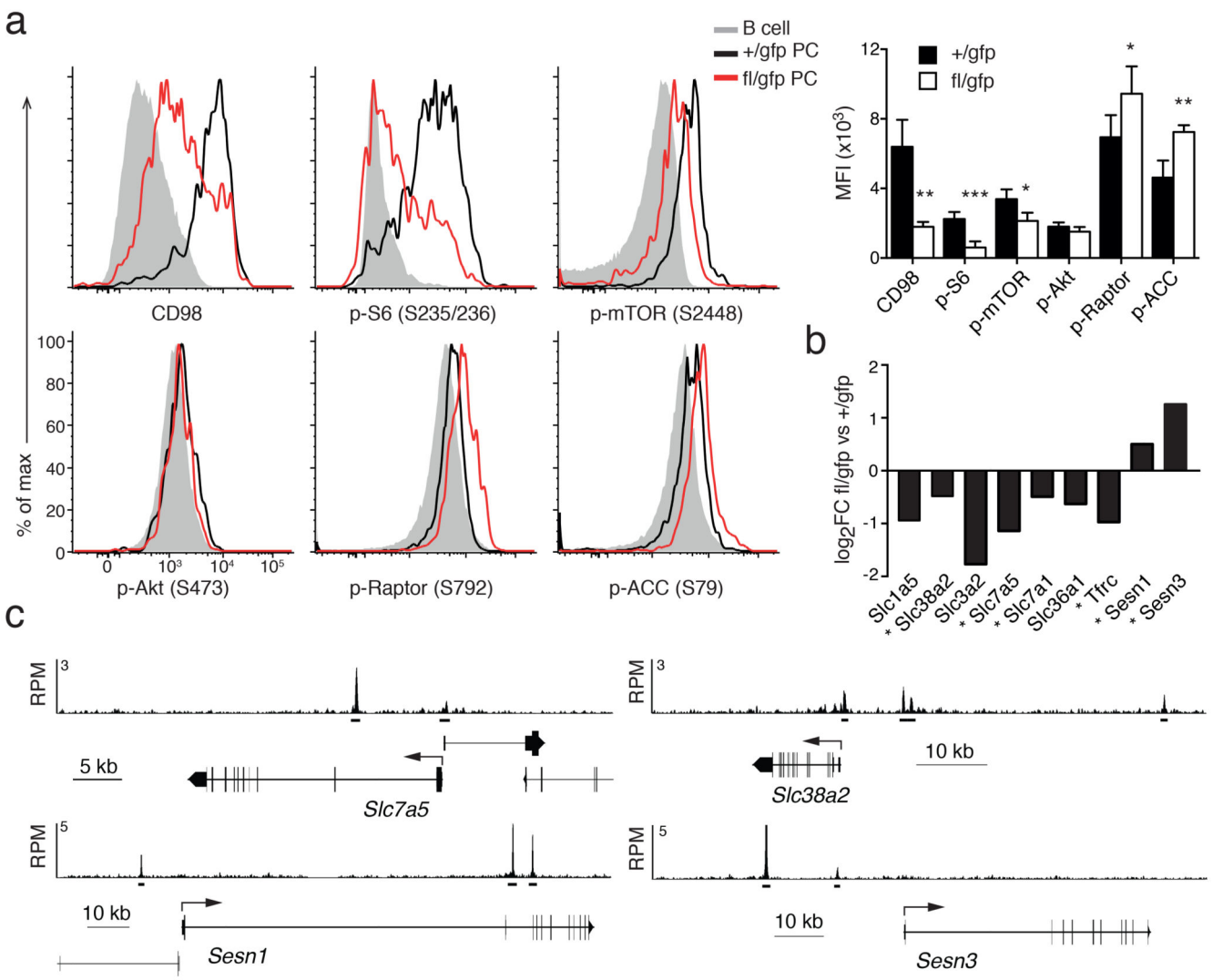

Figure 7.

Blimp-1 regulates the mTOR pathway. **(a)** Cytometry profiles of the expression of key components of the mTOR pathway, including the amino acid carrier CD98, and phosphorylation of mTOR, S6, Akt, Raptor and ACC in mature B cells ($B220^{hi}CD19^{hi}$) and PCs ($CD138^{+}$Blimp-1-GFP^{+}) from *Prdm1*$^{+/gfp}$Cre^{ERT2} (+/gfp) BM and *Prdm1*$^{fl/gfp}$Cre^{ERT2} (fl/gfp) BM PCs cells, 35 days after tamoxifen treatment. Right, graph shows the mean fluorescent index (MFI) ± S.D. of expression in PCs from 2 or more experiments for each antibody. *P* values compare the indicated groups using a paired *t*-test. * $P<0.05$, ** $P<0.01$, *** $P<0.005$. **(b)** RNA sequencing analysis showing fold changes in key genes upstream of the mTOR pathway in +/gfp and fl/gfp BM PCs analyzed as described in Fig. 2. * Indicates direct Blimp-1 target genes. **(c)** Blimp-1 binding at the *Slc7a5* (encoding a chain of CD98), *Slc38a2, Sesn1* and *Sesn3* genes in LPS-stimulated *Prdm1*$^{Bio/Bio}$*Rosa26*$^{BirA/BirA}$ tagged PBs. Blimp-1 peaks are shown together with the exon-intron structure of the gene and a scale bar in kilobases (kb). RPM, reads per million reads. Bars below the tracks indicate Blimp-1–binding regions identified by MACS peak calling.

Europe PMC Funders Author Manuscripts